Received: 16 September 2021 | Revised: 28 January 2022 | Accepted: 8 February 2022

DOI: 10.1111/ter.12584

RESEARCH ARTICLE

Terra Nova WILEY

Rotation at subduction margins: How complexity at fault-scale (the 2019 Albanian M_w 6.4 earthquake) mirrors the regional deformation

Giuseppe Pezzo[1] | Mimmo Palano[2] | Claudio Chiarabba[1]

[1]Istituto Nazionale di Geofisica e Vulcanologia, Osservatorio Nazionale Terremoti, Rome, Italy

[2]Istituto Nazionale di Geofisica e Vulcanologia, Osservatorio Etneo - Sezione di Catania, Catania, Italy

Correspondence
Giuseppe Pezzo, Istituto Nazionale di Geofisica e Vulcanologia, Via di Vigna Murata, 605, 00143 Rome, Italy.
Email: giuseppe.pezzo@ingv.it

Abstract

A variety of tectonic processes spread along the circum-Mediterranean orogenic belts driven by the convergence of major plates, episodes of slab retreat and lateral and vertical mantle flows. Here, we provide an updated view of crustal stress and strain-rate fields for the Albanides belt in the eastern Adria-Eurasia convergence boundary. We framed a new geodetic-based source model for the 2019 M_w6.4 Durrës earthquake in light of the regional deformation, propending for a transpressional west-dipping seismogenic fault. Our results highlight a fault-scale complexity which mirrors the long-time scale deformation of the Albanides plate boundary, where the rotation induced by the fast Hellenic rollback is accommodated also by transpression on inherited structures.

1 | INTRODUCTION

The kinematics of large earthquakes reflects, at a small temporal and spatial scale, the broad tectonic style of a region and the stress accumulation within the lithosphere. Coseismic displacements are the response of the crust with instantaneous dissipation of the energy stored during long interseismic periods. As a result, boundaries with complex plate interactions often feature heterogeneous earthquake fault ruptures. The severe complexity of processes along the circum-Mediterranean plate boundary is expressed by variable faulting mechanisms and earthquake depths, resulting from plate fragmentation and interaction between contiguous subduction arcs (Bennett et al., 2008; Carminati et al., 2012; Faccenna et al., 2014; Oldow et al., 2002; Reilinger & McClusky, 2011; Wortel & Spakman, 2001).

The November 26, 2019, M_w6.4 Durrës earthquake ideally describes such complexity of deformation. This earthquake is part of a seismic sequence spreading from late 2019 to early 2020 with 8 $M_w > 5$ reverse FMs with belt-perpendicular *P*-axes. Due to a rather sparse aftershock distribution and absence of primary surface coseismic ruptures (Papadopoulos et al., 2020), previous studies modelled the mainshock as either a low-angle ENE-dipping thrust (Caporali et al., 2020, Ganas et al., 2020, Papadopoulos et al., 2020; Vittori et al., 2021) or a SW-dipping back-thrust (Govorčin et al., 2020).

To solve the ambiguity, we face the problem by both local- and regional-scale approaches. We provided an updated frame of the current regional-scale stress and deformation for Albanides by using an extensive set of seismic and geodetic data and compute geodetic-based slip models for the mainshock, where two opposite dipping faults are equivalent from a statistical point of view. Joint interpretation of coseismic InSAR fringes pattern, interseismic and coseismic GNSS deformations, and available data and models, converges toward the activation of a blind transpressive regional fault, cutting the upper crust down to the basal thrust with a kinematic complexity consistent with the regional crustal stress where broad zones of transpression develop at the edge of a rotational deformation induced by the rollback of Hellenic subduction.

2 | BACKGROUND SETTING

The Albanian sector of Dinarides-Albanides-Hellenides (DAH; Figure 1) is a SW-vergent fold-and-thrust belt developed since Late Jurassic in the framework of the Africa-Eurasia plate convergence (Jolivet & Brun, 2010). The Albanides represent a large junction zone between the SW-verging Dinarides collisional belt (to the north) and the S-verging Hellenides (to the south) (Monopolis & Bruneton, 1982; Speranza et al., 1995; van Hinsbergen et al., 2005), in the transition from the Adriatic continental collision to the Aegean oceanic subduction (Halpaap et al., 2018).

The DAH is dissected into three main differently evolving sectors separated by prominent crustal-scale tectonic discontinuities (Figure 1). Dinarides and Albanides are separated by the NE–SW trending Shkoder-Peja transverse zone (SPTZ), a zone of dextral offset marked by gravimetric and magnetic anomalies (Bushati, 1997; Frasheri et al., 2009). This tectonic lineament has controlled, since the Early Miocene, the clockwise rotation of the Albanides with respect to the unrotated Dinarides (Speranza et al., 1995; van Hinsbergen et al., 2005). To the south, the right-lateral Cephalonia Transform Fault (CTF), located along the western edge of the Cephalonia-Lefkas Islands, separates the Albanides from the Hellenides (Monopolis & Bruneton, 1982).

The Albanides are formed by an external compressional and internal extensional domain. The former is made by envelops of the sedimentary cover deformed in uplifting anticlinal mountains and synclinal valleys related to NNW-striking, east-dipping thrusts and shallow conjugate west-dipping back-thrusts (Aliaj, 1997; Schmid et al., 2008) and secondary strike-slip faults that offset the anticlinal axes (Skrami & Aliaj, 1995). The latter is characterized by extension with N-S and NE–SW oriented normal faults whose Pliocene-to-recent activity have led to the formation of several intermountain basins and tectonic depressions (Aliaj, 1998).

Historically, the Albanides have experienced several strong M > 6 earthquakes (Grunthal et al., 2013; Stucchi et al., 2013), mostly in the period 1850–1915, concentrated along the external compressional domain. Such a pattern is also remarked by the spatial distribution of the instrumental seismicity (Figure 2a) clustering on low-angle NE-dipping thrusts (e.g., the M_w7.1 1979 Montenegro earthquake; Baker et al., 1997) and occasionally on high-angle back-thrusts (e.g., Copley et al., 2009; Louvari et al., 2001). The spatial distribution of focal mechanisms (FMs) shows homogeneous zones with normal faulting solutions prevailing along the internal extensional domain and reverse (~65%) and strike-slip (~35%) faulting in the external domain (Figure 2a).

3 | DATA AND RESULTS

Here, firstly we estimated the crustal stress and strain patterns for the Albanides, to get a reference tectonic framework, and lastly, we modelled the available InSAR and GNSS data to constrain the causative source of the 2019 M_w6.4 Durrës earthquake.

Significance Statement

We provide a novel interpretation of long- and short-term tectonic processes interaction along the Albanides plate boundary by computing the regional stress and strain-rate fields and a geodetic model for the 2019 Durrës earthquake. In particular, we explain the Durres earthquake that occured on a relatively high angle inherited west-dipping fault, accommodating transpression generated by rotation induced by slab rollback.

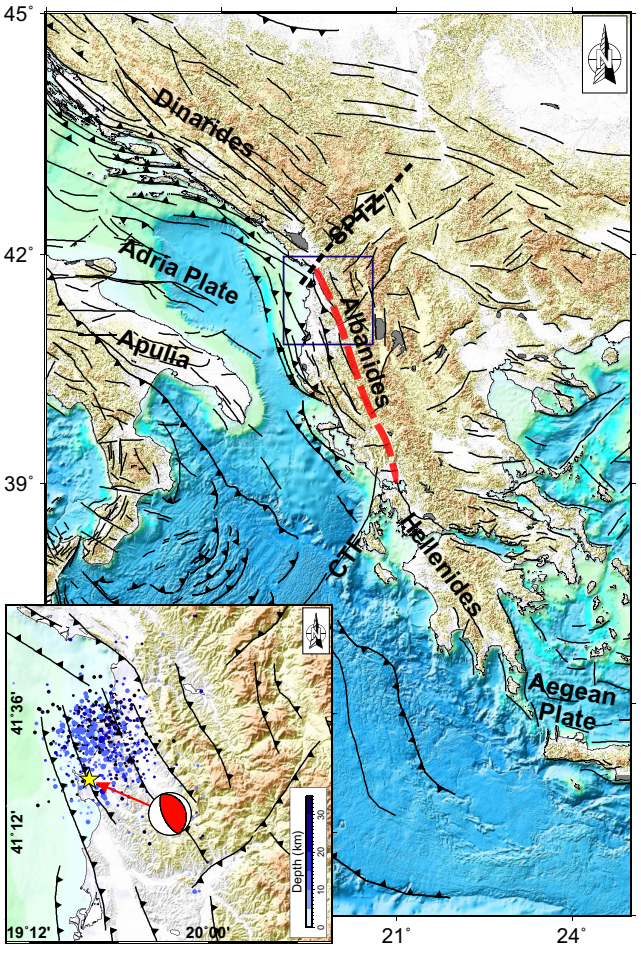

FIGURE 1 Regional tectonic framework showing major orogens and main faults (taken from https://edsf13.ingv.it/). Abbreviations: CTF, Cephalonia transform fault; SPTZ, Shkoder-Peja transverse zone. The blue polygon represents the area mapped in the inset. The inset shows the $M > 2$ events of the Durrës earthquake sequence (www.isc.ac.uk) along with the FM associated to the M_w6.4 2019 November 26 event (https://earthquake.usgs.gov/earthquakes/eventpage/us70006d0m/pager). The shallow W-dipping Vore back-thrust (Vb) is also reported

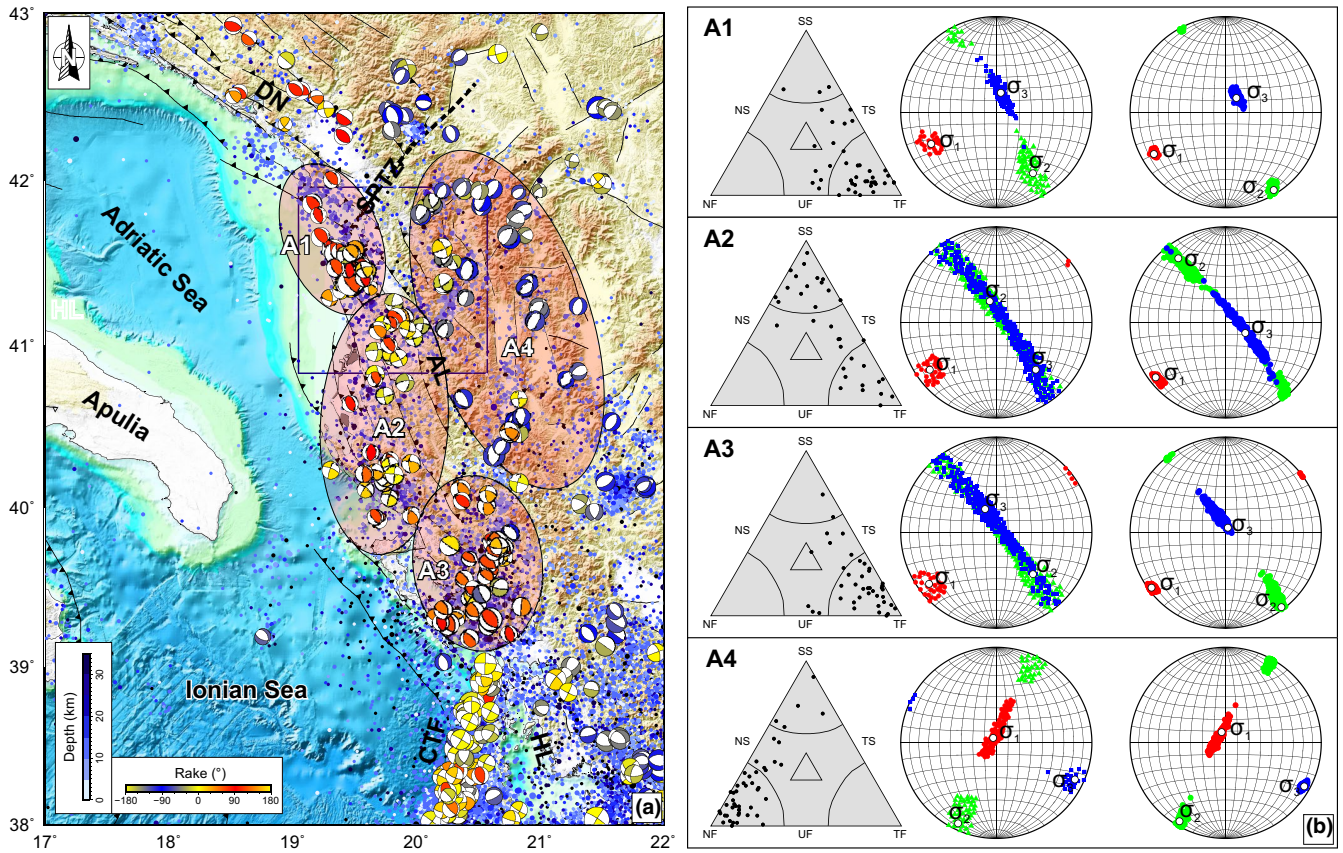

FIGURE 2 (a) Lower hemisphere, equal area projection for FMs ($M_w \geq 3.6$) compiled in this study from online catalogues (http://rcmt2.bo.ingv.it, http://www.eas.slu.edu/eqc/eqc_mt/MECH.EU). FMs are coloured according to rake: red indicates thrust faulting, blue is normal faulting and yellow is strike-slip faulting. A1, A2, A3 and A4 represent the datasets used for the stress tensor inversions. The instrumental crustal seismicity ($M \geq 3.0$) occurring since 1950 (www.isc.ac.uk) is reported in the background. Abbreviations: AL, Albanides; CTF, Cephalonia transform fault; DN, Dinarides; HL, Hellenides; SPTZ, Shkoder-Peja transverse zone. (b) Frohlich (1992) ternary diagrams (on the left) and graphic output of the stress tensor inversion results were obtained with M84 (to the centre) and V14 (on the right) methods for each dataset. The Frolich diagram is divided into faulting styles: NF is normal faulting, NS is normal and strike-slip faulting, SS is strike-slip faulting, TS is thrust and strike-slip faulting, TF is thrust faulting and U is undefined faulting

3.1 | Stress computation

We subdivided the investigated region into four contiguous zones based on lateral continuity of faults and lineaments and consistency in FMs. The external domain has been divided into three different zones (A1, A2, A3, Figure 2a) while only a zone (A4 in Figure 2) has been defined for the internal domain. Each zone contains an adequate number (>30; Table S1) of FMs to properly constrain the related stress field parameters. We performed the stress tensor inversion to get the principal stress axes orientations ($\sigma_1 > \sigma_2 > \sigma_3$) and the stress ratio value (R) that gives indications on how close in magnitude the principle axes are. Due to the tectonic complexity of the study area, we used the method M84 (Michael, 1984, 1987) since it provides well-constrained solutions also without a priori information on the preferred fault plane. Moreover, to check results robustness, we also used the approach V14 (Vavryčuk, 2014), in which the fault plane is chosen by an instability constraint and the optimal stress tensor is determined in iterations (see Supporting information). Comparison of best-fit solutions from the M84 and V14 methods (Figure 2b) shows that the orientations of the stress axes are generally consistent, and the different assumptions do not affect the solutions (see Table S1). Anyway, the two methods slightly differ in the estimated confidence limits, being larger for M84.

The results show that A1, A2 and A3 regions are characterized by a compressional stress regime with a well-constrained subhorizontal SW-plunging σ_1. The orientations of σ_2 and σ_3 are well constrained only for A1, while their 95% confidence limits overlap for A2 and A3, on the plane perpendicular to σ_1, suggesting that they are approximately equal in magnitude ($R > 0.8$). The magnitude proximity of σ_2 and σ_3 is also remarked by the flip between the two stress axes for the solutions in A2 (Figure 2b) and by the equal mixture of reverse and strike-slip solutions. The A4 region is characterized by an extensional regime with a well-constrained subhorizontal σ_3, equally resolved by both methods. Although confidence limits of σ_2 and σ_1 do not overlap, the $R < 0.2$ value, coupled with the σ_2 and σ_1 dispersion on the plane perpendicular to σ_3 implies a slight coexistence of both normal and strike-slip mechanisms. Our estimated stress fields well match the ones estimated by local field data (e.g., Graham

et al., 2006; Lacombe et al., 2009) as well as the regional pattern reported in Heidback et al. (2018).

3.2 | GNSS velocity and strain computation

We analysed an extensive GNSS dataset by using the GAMIT/GLOBK software (Herring et al., 2018) to estimate a consistent set of velocities in a Eurasian frame (Palano et al., 2017). To improve the spatial density of the geodetic velocity field (Figure 3a), we integrated our solutions with those reported in the recent literature (Chiarabba & Palano, 2017; D'Agostino et al., 2020; England et al., 2016). We estimated the horizontal strain rates on a regular 0.25° × 0.25° grid (Figure 3b) by using the VISR code (Shen et al., 2015) (see Supporting information).

The main feature of the regional velocity field (Figure 3a) is given by the clockwise rotation of the internal Albanides domain with rates increasing southward (~10 mm/a at the Albanides–Hellenides boundary and more than 20 mm/a in northern Hellenides), accommodated by the NE–SW-trending normal faults (Figure 1). Few coastal stations along the external domain move toward NNE with rates of 3–4 mm/a showing a variable coupling with the motion of Apulia (~5 mm/a). This pattern highlights a complex deformation where the Adria-Eurasia convergence is accommodated in a narrow NNW-striking belt (external domain) on thrusts and associated structures (back-thrusts and transpressive steep structures). The pattern of crustal stretching and shortening strain rates (Figure 3b) well match the spatial distribution of both normal and reverse faults (Figure 1) and FMs (Figure 2) already discussed for both the Albanides domains. The internal domain is characterized by a crustal stretching of ~45 nanostrains (on average) with extensional axes orthogonal to the NE–SW normal faults, while the internal domain is characterized by a crustal shortening of ~55 nanostrains with NE–SW contractional axes, evidencing the transpressive nature of the Adria-Eurasia convergence along the Albanides.

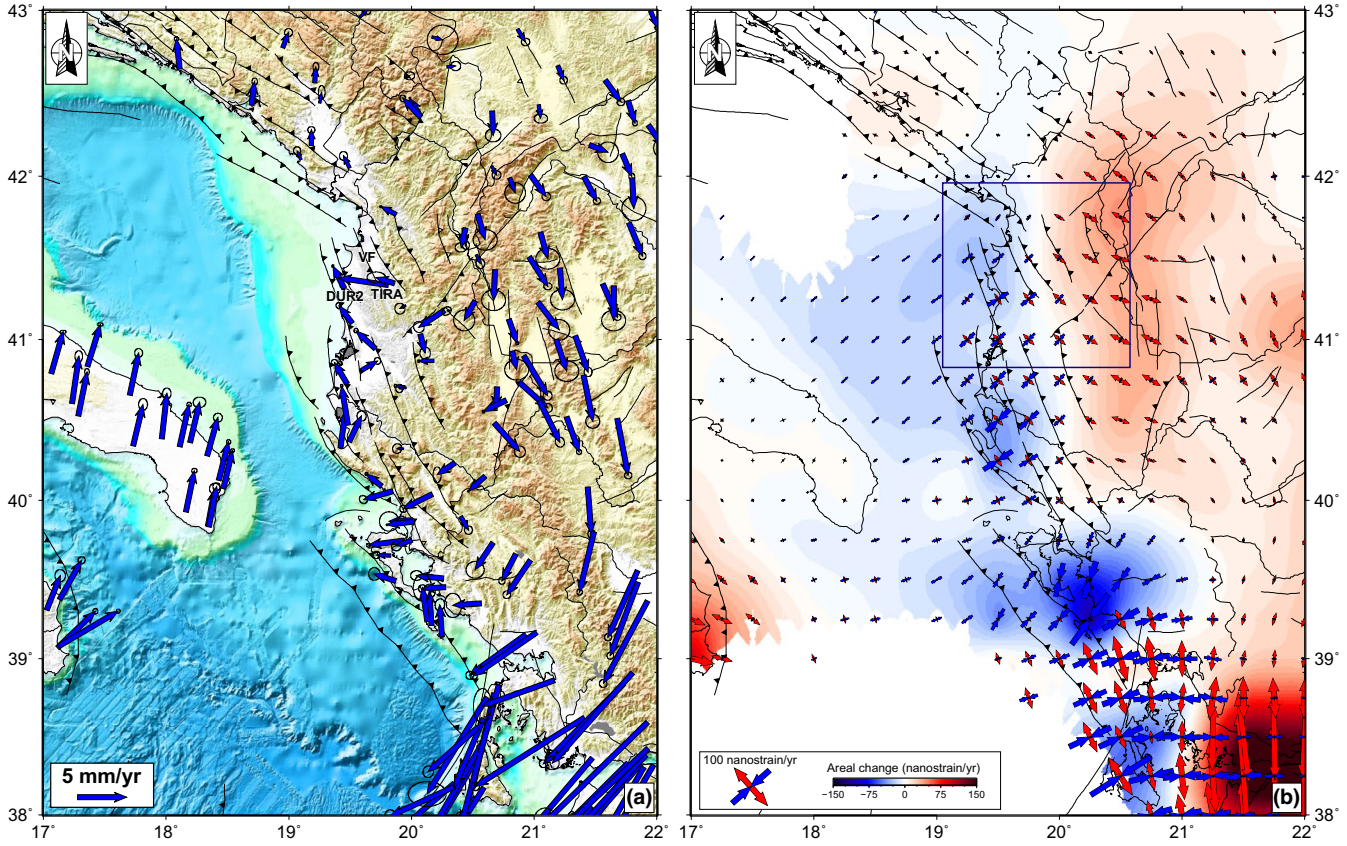

FIGURE 3 (a) GNSS velocities and 95% confidence ellipses in a fixed Eurasia frame. DUR2 and TIRA are GNSS stations discussed in the maintex. VF, Vore back-thrust. (b) Geodetic strain-rate parameters: background colour shows the rate of spatial change while arrows represent the greatest extensional (red) and contractional (blue) horizontal strain rates. Uncertainties related to the horizontal strain rates are reported as black bars. The blue polygon represents the area mapped in Figure 4a

FIGURE 4 (a) Asc. and (d) Desc. 2019 Nov; 26 coseismic displacements, satellite flight paths and LoS are represented. Synthetic LoS displacements from E- and W-dipping models are reported in panels (b), (c), (e) and (f). The horizontal observed (black) and modelled (blue) GNSS coseismic vectors are reported in panels (b) and (c) for E- and W-dipping models respectively. In panels (e) and (f) the corresponding GNSS vertical displacements. Panels (g), (h) and (i) represent the slip distributions, the slip vectors (on a 1 × 1 km grid) and focal mechanisms for E-dipping best-fit solution; panels (j), (k) and (l) are for W-dipping one

(a) Obs. Asc. 20191114–20191126

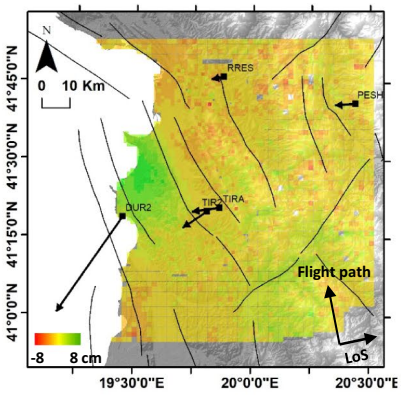

(b) E-dipping Model

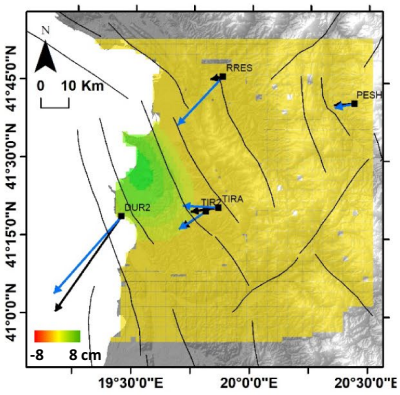

(c) W-dipping Model

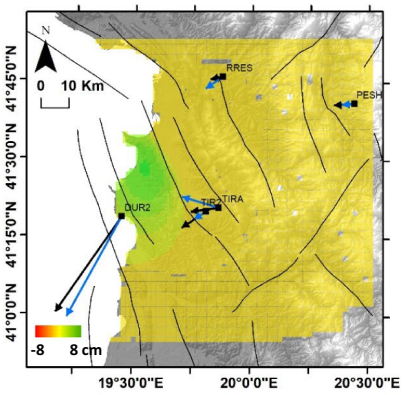

(d) Obs. Desc. 20191125-20191201

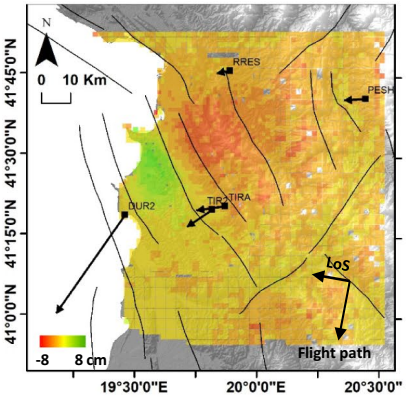

(e) E-dipping Model

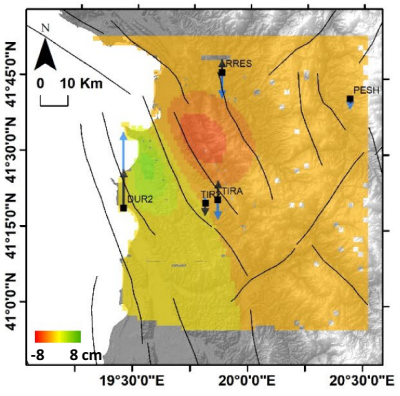

(f) W-dipping Model

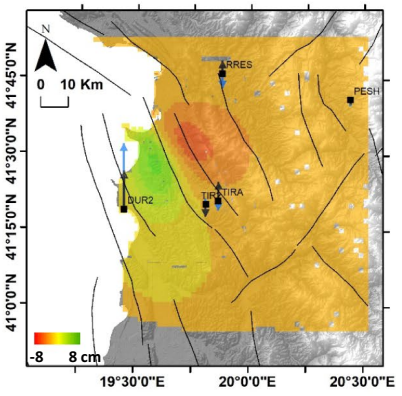

(g) E-dipping Model – Slip distr.

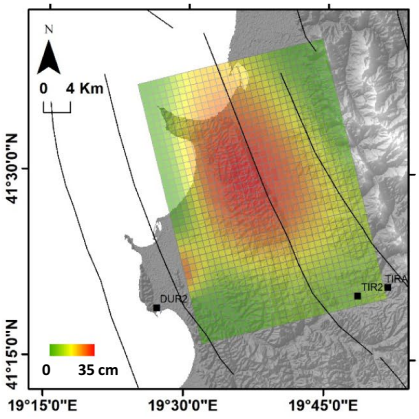

(h) E-dipping Model – Slip distr.

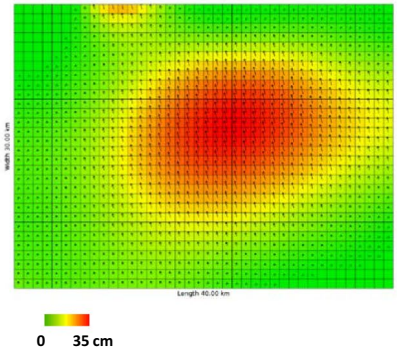

(i) E-dipping Model – Focal Mec.

Magnitude = 6.4
Strike = 346°
Dip = 18°
Rake = 103°

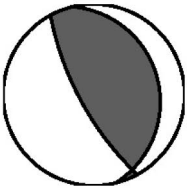

(j) W-dipping Model – Slip distr.

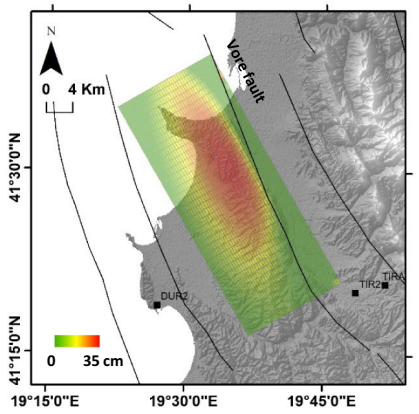

(k) W-dipping Model – Slip distr.

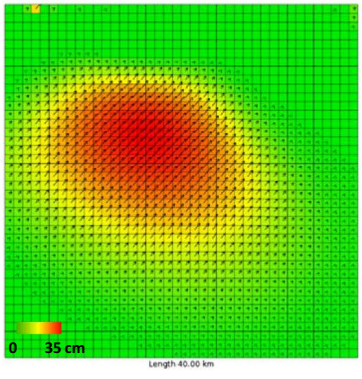

(l) W-dipping Model – Desc. res.

Magnitude = 6.4
Strike = 150°
Dip = 66°
Rake = 49°

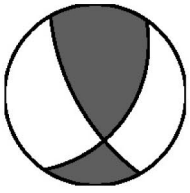

3.3 | The M_w6.4 source model

GNSS coseismic displacements are estimated by differencing the average site position of our GAMIT/GLOBK solutions in the 2 days before and after the earthquake occurrence. We detected significant displacements at TIRA, TIR2 and DUR2 stations, because of their proximity to the epicentre (Figure 4). Using the Sarscape software, we processed two ascending and one descending Sentinel-1 SAR pairs spanning the periods November 14–20, November 20–26 and November 11 to December 1 (Figure S2) to obtain 15 × 15 m coseismic interferograms. Line of sight (LoS) displacement maps are in very good agreement with each other and depict a large uplift area of about 8 cm. The fringe pattern sharply changes in concomitance with the surface expression of the Vore back-thrust, bordering the NNW trending mountain ridge, while they appear larger and smoother toward the south-west (Figures S2 and S5). To model the seismic source, we performed a preliminary non-linear inversion to define fault geometry and kinematics, followed by a linear inversion for the slip distribution. We jointly inverted GNSS and SAR data by using Okada's (1985) formalism. We used only one ascending dataset to avoid redundancy and imbalance between the two LoS, favouring the smallest temporal baseline pair. We explored both geometries during the first non-linear step and then compared the slip-distributions (Figure 4). The E-dipping solution (strike 346°) requires displacements on a low (18°) angle plane at depth > 10 km to fit GNSS data at close stations (details in Supporting information). Although both models similarly reproduce the observed coseismic displacements (Figure S6), the W-dipping model (strike 150°, dip 66°) performs decisively better at the RRES station. For the W-dipping model, most of the coseismic displacement at DUR2 station is given by the strike-slip component (Figure 5).

4 | DISCUSSION

Strain rates from GNSS data and stress tensor inversions highlight a kinematics complexity at the northern continental margin of the oceanic Hellenic subduction. Reverse FMs prevail in a ~300 km long portion of the coastal area, coexisting, while locally interrupted, by strike-slip fault zones. Compression is replaced by extension in the internal domain, where the principal stress axes maintain the same direction and flip in absolute and relative magnitude. The progressive increase in strain-rate from north to south is consistent with the subduction rollback, being the dominant shaping role as also proposed by Handy et al., 2019. Rotation induced by the NNW motion of Apulian and Dinarides with respect to the SW-verging motion of the Hellenides give rise to the development of broadly compressive (A1 and A3), transpressional (A2 and CTF) and extensional structures (A4), accommodated north by the SPTZ, and south by the CTF. The latter is very clear and decouples the margin of the fast retreating slab with respect to the continental Adria-Eurasia convergence. Conversely, transpression in A2 and

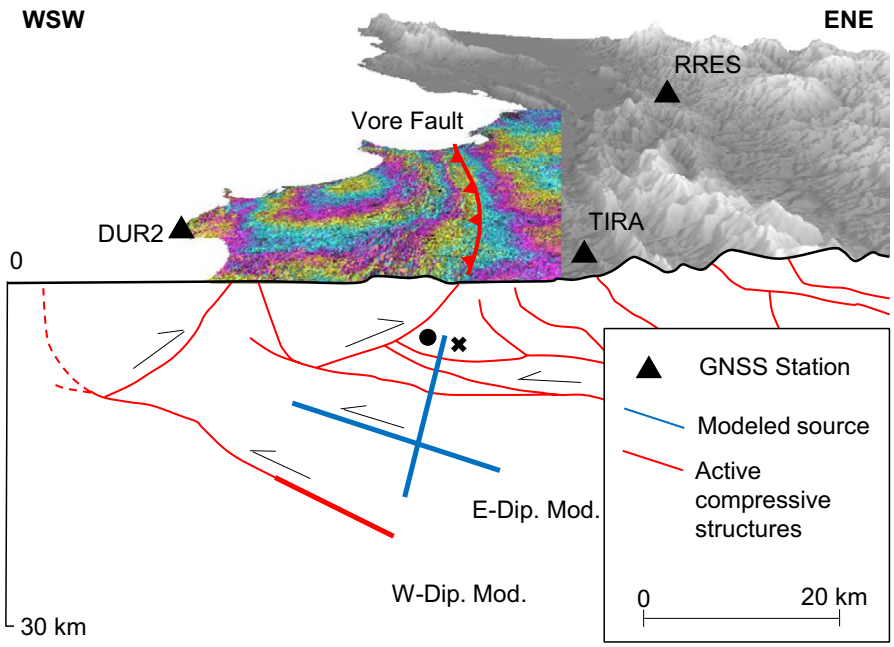

FIGURE 5 In the upper part, we provide a 3D view of the coseismic deformation spreading the 20 191 120–20 191 126 ascending interferograms on the digital elevation model. GNSS stations and the Vore fault trace are also reported. Underneath, a schematic WSW-ENE section of the Durrës area, modified after Vittori et al. (2021) and reference therein. Major active tectonic structures (in red) depict a thrust and back-thrust setting with a poorly constrained frontal thrust surfacing onshore. Both E- and W-dipping models (in blue) fit the coseismic deformation. However, our preferred W-dipping model reveals a transpressive kinematic, characterized by 46% of left-lateral strike-slip mechanism, as represented in the sketch

partially in A1 disperse on a broad zone where σ_1 is subhorizontal (Figure 2b) while σ_2 and σ_3 are closer in magnitude and may easily flip, giving rise to consistent reverse or strike-slip faulting mechanisms. Embedded in between these two main systems, a broad structure emerges with prevalent reverse solutions and subhorizontal σ_1 (A3 region).

On November 26, 2019, an earthquake occurred at the SW termination of the SPTZ were reverse and strike-slip FMs alternate and overlap (A1). Here, the southward strike rotation of the SPTZ implies a relevant reverse component in long- and short-term kinematics. Previous geodetic-based source models presented either E- or W-dipping solutions, neglecting the co- and interseismic strike-slip components in deformation and geological-structural patterns, as shown by the strain-rate field, where a clear transpression in the earthquake source area is evident (Figure 3b). Ganas et al. (2020) and Vittori et al. (2021) favour an E-dipping fault, consistent with the activation of a deep-blind-low-angle thrust. Govorčin et al. (2020) discussed both geometries and supported the activation of a blind-high-angle back-thrust, namely the Vore back-thrust. The east-dipping plane, with a great depth of 20 km and low dip angle, is not an obvious feature of the regional structural setting (see also Vittori et al., 2021), decoupled from the shallower east-verging thrust system and poorly known or constrained. Our preferred solution consists of a major transpressive kinematics (46% of strike-slip component) on a blind plane whose surface expression coincides with the mapped Vore back-thrust (Basili et al., 2013). This oblique solution similarly fits the overall data, while better explaining geodetic data at the station RRES and the asymmetry of the InSAR fringe pattern (denser near the Vore back-thrust trace). Moreover, InSAR fringes and slip distribution highlight how the coseismic uplift is coincident and confined along the compressive ridge, suggesting a repeating activation of the fault. A further indication comes from the interseismic GNSS velocities (Figure 3a) showing a relative compression between DUR2 and TIRA stations (Figure 3a), inconsistent with both points being in a solidly deforming block, i.e., the fault hanging wall of the deep east-dipping plane.

Therefore, we are attracted to consider the W-dipping transpressive fault as the causative source for the 2019 earthquake. Our model resolves an even higher strike-slip component, consistent with the regional stress (A1 in Figure 2b) and requires a slip down to a depth of 12–15 km, suggesting an inherited, regional-scale transpressive fault. An interesting scenario is given by the interaction with the deeper, external thrust and a possible simultaneous activation of the two faults. Complex faulting along more than one plane is documented in many large compressional earthquakes, like the 2008 Pakistan, the 2016 and 2010–2011 New Zealand seismic sequences (Atzori et al., 2012; Cesca et al., 2017; Pezzo et al., 2014). Even more speculative is the hypothesis that part of the slip on one of the two planes occurred aseismically. However, differently from the other examples, the spatial overlapping of the two sources leaves such an issue unsolvable for the 2019 Albania case.

The 2019 Durrës earthquake is replicating, at the scale of seconds and tens of kilometres, the long-term and regional transpression in a sector of the Albanides formed by the delicate equilibrium between the S-ward suction due to the fast Hellenic slab retreat (few centimetres) and the slow convergence in the Dinarides (few millimetres). In our model, the dominant engine and the differential velocity of retreat induce transpression at the northern edge of the system, mirrored by the M_w6.4 earthquake faulting mechanism. The rotation (Figure 2a) creates a series of strike-slip zones, similar to the corridors bordering the Pannonian basin (Csontos et al., 1992; Marko et al., 2017; Tari et al., 1992), with lateral irregularities promoting the development of compressional positive mega-flower zones (A3). The development of similar structures at the edge of fast retreating slabs could be a consistent pattern that develops in compressional margins worldwide.

5 | CONCLUSIONS

The 2019 M_w6.4 Durrës earthquake enclosed in a single rupture lasted only a few seconds all the tectonics complexity that spread on a thousand-kilometre-long margin and ka time evolution. The rotation induced by slab-retreat suction induces transpression at the edge of the subduction with the coexistence of reverse and strike-slip mechanisms. Our favoured causative source is a transpressive blind W-dipping fault. Its oblique kinematics and SE-ward continuity, and stress transfer from the earthquake, could imply an increased expectation of earthquakes in the Tirana region, requiring an update of seismogenic source catalogues for earthquake hazards.

ACKNOWLEDGEMENT

We thank C. Tolomei and S. Atzori for supporting the SAR data processing and inversion. Sentinel-1 data are copyrighted by Copernicus. We also thank S. Tavani and an anonymous reviewer for their very helpful comments.

DATA AVAILABILITY STATEMENT

The data that support the findings of this study are openly available in DATA-SHARING_Pezzo_et_al_Terra_Nova at https://drive.google.com/drive/folders/1Xj_Wxo3HQczi7xVuvoGB-XFYy5iNqxu_?usp=sharing.

REFERENCES

Aliaj, S. (1997). Alpine geological evolution of Albania. *Albanian Journal of Natural and Technology Sciences*, *3*, 69–81.

Aliaj, S. (1998). Neotectonic structure of Albania. *Albanian Journal of Natural and Technology Sciences*, *4*, 15–42.

Atzori, S., Tolomei, C., Antonioli, A., Merryman Boncori, J. P., Bannister, S., Trasatti, E., Pasquali, P., & Salvi, S. (2012). The 2010-2011 Canterbury, New Zealand, seismic sequence: multiple source analysis from InSAR data and modeling. *Journal of Geophysical Research*, *117*, B08305. https://doi.org/10.1029/2012JB009178

Baker, C., Hatzfeld, D. L., Lyon-Caen, H., Papadimitriou, E., & Rigo, A. (1997). Earthquake mechanisms of the Adriatic Sea and Western Greece: Implications for the oceanic subduction-continental collision transition. *Geophysical Journal International*, *131*(3), 559–594.

Basili, R., Kastelic, V., Demircioglu, M. B., Garcia Moreno, D., Nemser, E. S., Petricca, P., … Wössner J. (2013). *The European Database of Seismogenic Faults (EDSF) compiled in the framework of the Project*

SHARE. Retrieved from http://diss.rm.ingv.it/share-edsf/, 10.6092/INGV.IT-SHARE-EDSF.

Bennett, R. A., Hreinsdóttir, S., Buble, G., Bašić, T., Bačić, Z., Marjanović, M., … Cowan, D. (2008). Eocene to present subduction of southern Adria mantle lithosphere beneath the Dinarides. *Geology*, *36*(1), 3–6.

Bushati, S., 1997. Geomagnetic Field of Albania, Magnetic Map Monography, Center of Geophysical and Geochemical Investigation. Albanian Geological Survey.

Caporali, A., Floris, M., Chen, X., Nurce, B., Bertocco, M., & Zurutuza, J. (2020). The November 2019 seismic sequence in Albania: Geodetic constraints and fault interaction. *Remote Sensing*, *12*(5), 846. https://doi.org/10.3390/rs12050846

Carminati, E., Lustrino, M., & Doglioni, C. (2012). Geodynamic evolution of the central and western Mediterranean: Tectonics vs. igneous petrology constraints. *Tectonophysics*, *579*, 173–192. https://doi.org/10.1016/j.tecto.2012.01.026

Cesca, S., Zhang, Y., Mouslopoulou, V., Wang, R., Saul, J., Savage, M., … Dahm, T. (2017). Complex rupture process of the Mw July 8, 2016, Kaikoura earthquake, New Zealand, and its aftershock sequence. *Earth and Planetary Science Letters*, *478*, 110–120.

Chiarabba, C., & Palano, M. (2017). Progressive migration of slab breakoff along the southern Tyrrhenian plate boundary: Constraints for the present day kinematics. *Journal of Geodynamics*, *105*, 51–61. https://doi.org/10.1016/j.jog.2017.01.006

Copley, A., Boait, F., Hollingsworth, J., Jackson, J., & McKenzie, D. (2009). Subparallel thrust and normal faulting in Albania and the roles of gravitational potential energy and rheology contrasts in mountain belts. *Journal of Geophysical Research: Solid Earth*, *114*, B05407. https://doi.org/10.1029/2008JB005931

Csontos, L., Nagymarosy, A., Horváth, F., & Kovac, M. (1992). Tertiary evolution of the Intra-Carpathian area: A model. *Tectonophysics*, *208*(1–3), 221–241.

D'Agostino, N., Métois, M., Koci, R., Duni, L., Kuka, N., Ganas, A., … Kandić, R. (2020). Active crustal deformation and rotations in the southwestern Balkans from continuous GPS measurements. *Earth and Planetary Science Letters*, *539*, 116246. https://doi.org/10.1016/j.epsl.2020.116246

England, P., Houseman, G., & Nocquet, J. M. (2016). Constraints from GPS measurements on the dynamics of deformation in Anatolia and the Aegean. *Journal of Geophysical Research: Solid Earth*, *121*(12), 8888–8916. https://doi.org/10.1002/2016JB013382

Faccenna, C., Becker, T. W., Auer, L., Billi, A., Boschi, L., Brun, J. P., … Serpelloni, E. (2014). Mantle dynamics in the Mediterranean. *Reviews of Geophysics*, *52*(3), 283–332. https://doi.org/10.1002/2013RG000444

Frasheri, A., Bushati, S., & Bare, V. (2009). Geophysical outlook on structure of the Albanides. *Journal of the Balkan Geophysical Society*, *12*(1), 9–30.

Frohlich, C. (1992). Triangle diagrams: Ternary graphs to display similarity and diversity of earthquake focal mechanisms. *Physics of the Earth and Planetary Interiors*, *75*, 193–198. https://doi.org/10.1016/0031-9201(92)90130-n

Ganas, A., Elias, P., Briole, P., Cannavo, F., Valkaniotis, S., Tsironi, V., & Partheniou, E. I. (2020). Ground deformation and seismic fault model of the M6.4 Durres (Albania) Nov. 26, 2019 earthquake, based on GNSS/INSAR observations. *Geosciences*, *10*, 210. https://doi.org/10.3390/geosciences10060210

Govorčin, M., Wdowinski, S., Matoš, B., & Funning, G. J. (2020). Geodetic source modeling of the 2019 Mw 6.3 Durrës, Albania, Earthquake: Partial rupture of a blind reverse fault. *Geophysical Research Letters*, *47*(22), e2020GL088990. https://doi.org/10.1029/2020GL088990

Graham Wall, B. R., Girbacea, R., Mesonjesi, A., & Aydin, A. (2006). Evolution of fracture and fault-controlled fluid pathways in carbonates of the Albanides fold-thrust belt. *AAPG Bulletin*, *90*(8), 1227–1249.

Grünthal, G., Wahlström, R., & Stromeyer, D. (2013). The SHARE European Earthquake Catalogue (SHEEC) for the time period 1900-2006 and its comparison to the European-Mediterranean Earthquake Catalogue (EMEC). *Journal of Seismology*, *17*(4), 1339–1344.

Halpaap, F., Rondenay, S., & Ottemöller, L. (2018). Seismicity, deforma,tion, and metamorphism in the Western Hellenic Subduction Zone: New constraints from tomography. *Journal of Geophysical Research: Solid Earth*, *123*(4), 3000–3026. https://doi.org/10.1002/2017JB015154

Handy, M. R., Giese, J., Schmid, S. M., Pleuger, J., Spakman, W., Onuzi, K., & Ustaszewski, K. (2019). Coupledcrust-mantle response to slab tearing, bending, and rollback along the Dinaride-Hellenide orogen. *Tectonics*, *38*, 2803–2828. https://doi.org/10.1029/2019TC005524

Heidbach, O., Rajabi, M., Cui, X., Fuchs, K., Müller, B., Reinecker, J., Reiter, K., Tingay, M., Wenzel, F., Xie, F., Ziegler, M. O., Zoback, M.-L., & Zoback, M. D. (2018). The World Stress Map database release 2016: Crustal stress pattern across scales. *Tectonophysics*, *744*, 484–498. https://doi.org/10.1016/j.tecto.2018.07.007

Herring, T. A., King, R. W., Floyd, M. A., & McClusky, S. C. (2018). *Introduction to GAMIT/GLOBK*, *release 10.70*. Massachusetts Institute of Technology.

Jolivet, L., & Brun, J. P. (2010). Cenozoic geodynamic evolution of the Aegean. *International Journal of Earth Sciences (Geol Rundsch)*, *99*, 109–138. https://doi.org/10.1007/s00531-008-0366-4

Lacombe, O., Malandain, J., Vilasi, N., Amrouch, K., & Roure, F. (2009). From paleostresses to paleoburial in fold–thrust belts: Preliminary results from calcite twin analysis in the Outer Albanides. *Tectonophysics*, *475*(1), 128–141.

Louvari, E., Kiratzi, A., Papazachos, B., & Hatzidimitriou, P. (2001). Fault-plane solutions determined by waveform modeling confirm tectonic collision in the Eastern Adriatic. *Pure and Applied Geophysics*, *158*(9), 1613–1637.

Marko, F., Andriessen, P. A., Tomek, Č., Bezák, V., Fojtíková, L., Bošanský, M., … Reichwalder, P. (2017). Carpathian Shear Corridor-a strike-slip boundary of an extruded crustal segment. *Tectonophysics*, *703*, 119–134.

Michael, A. J. (1984). Determination of stress from slip data: Faults and folds. *Journal of Geophysical Research: Solid Earth*, *89*(B13), 11517–11526. https://doi.org/10.1029/JB089iB13p11517

Michael, A. J. (1987). Use of focal mechanisms to determine stress: A control study. *Journal of Geophysical Research: Solid Earth*, *92*(B1), 357–368. https://doi.org/10.1029/JB092iB01p00357

Monopolis, D., & Bruneton, A. (1982). Ionian Sea (Western Greece): Its structural outline deduced from drilling and geophysical data. *Tectonophysics*, *83*(3–4), 227–242. https://doi.org/10.1016/0040-1951(82)90020-8

Okada, Y. (1985). Surface deformation due to shear and tensile faults in a half-space. *Bulletin of the Seismological Society of America*, *75*(4), 1135–1154.

Oldow, J. S., Ferranti, L., Lewis, D. S., Campbell, J. K., d'Argenio, B., Catalano, R., … Aiken, C. L. V. (2002). Active fragmentation of Adria, the north African promontory, central Mediterranean orogen. *Geology*, *30*(9), 779–782.

Palano, M., Piromallo, C., & Chiarabba, C. (2017). Surface imprint of toroidal flow at retreating slab edges: The first geodetic evidence in the Calabrian subduction system. *Geophysical Research Letters*, *44*(2), 845–853. https://doi.org/10.1002/2016GL071452

Papadopoulos, G. A., Agalos, A., Carydis, P., Lekkas, E., Mavroulis, S., & Triantafyllou, I. (2020). The November 26, 2019 Mw 6.4 Albania Destructive Earthquake. *Seismological Society of America*, *91*(6), 3129–3138. https://doi.org/10.1785/0220200207

Pezzo, G., Merryman Boncori, J. P., Atzori, S., Antonioli, A., & Salvi, S. (2014). Deformation of the western Indian Plate boundary: insights from differential and multi-aperture InSAR data inversion for the 2008 Baluchistan (Western Pakistan) seismic sequence. *Geophysical Journal International*, *198*(1), 25–39. https://doi.org/10.1093/gji/ggu106

Reilinger, R., & McClusky, S. (2011). Nubia-Arabia-Eurasia plate motions and the dynamics of Mediterranean and Middle East tectonics. *Geophysical Journal International*, *186*(3), 971–979.

Schmid, S. M., Bernoulli, D., Fügenschuh, B., Matenco, L., Schefer, S., Schuster, R., … Ustaszewski, K. (2008). The Alpine-Carpathian-Dinaridic orogenic system: Correlation and evolution of tectonic units. *Swiss Journal of Geosciences*, *101*(1), 139–183.

Shen, Z. K., Wang, M., Zeng, Y., & Wang, F. (2015). Optimal interpolation of spatially discretized geodetic data. *Bulletin of the Seismological Society of America*, *105*(4), 2117–2127. https://doi.org/10.1785/0120140247

Skrami J. and Aliaj S., 1995. Thrusts and back-thrusts on Preadriatic Depression (Albania) deduced from exploration seismics. Geol. Soc. Greece No 4- Proc. of the XV Congress of the Carpatho- Balkan Geological Association, 1139–1143.

Speranza, F., Islami, I., Kissel, C. and Hyseni, A., 1995. Paleomagnetic evidence for Cenozoic clockwise rotation of the external Albanides. *Earth and Planetary Science Letters*, *129*(1–4), 121–134. https://doi.org/10.1016/0012-821X(94)00231-M.

Stucchi, M., Rovida, A., Capera, A. G., Alexandre, P., Camelbeeck, T., Demircioglu, M. B., … Giardini, D. (2013). The SHARE European earthquake catalogue (SHEEC) 1000–1899. *Journal of Seismology*, *17*(2), 523–544.

Tari, G., Horváth, F., & Rumpler, J. (1992). Styles of extension in the Pannonian Basin. *Tectonophysics*, *208*(1–3), 203–219.

Van Hinsbergen, D. J. J., Langereis, C. G., & Meulenkamp, J. E. (2005). Revision of the timing, magnitude and distribution of Neogene rotations in the western Aegean region. *Tectonophysics*, *396*(1–2), 1–34. https://doi.org/10.1016/j.tecto.2004.10.001

Vavryčuk, V. (2014). Iterative joint inversion for stress and fault orientations from focal mechanisms. *Geophysical Journal International*, *199*(1), 69–77. https://doi.org/10.1093/gji/ggu224

Vittori, E., Blumetti, A. M., Comerci, V., Di Manna, P., Piccardi, L., Gega, D., & Hoxha, I. (2021). Geological effects and tectonic environment of the November 26, 2019, M w 6.4 Durres earthquake (Albania). *Geophysical Journal International*, *225*(2), 1174–1191.

Wortel, M. J. R., & Spakman, W. (2001). Subduction and slab detachment in the Mediterranean-Carpathian region. *Science*, *291*, 1910–1917. https://doi.org/10.1126/science.290.5498.1910

SUPPORTING INFORMATION

Additional supporting information may be found in the online version of the article at the publisher's website.

DataS 1

How to cite this article: Pezzo, G., Palano, M., & Chiarabba, C. (2022). Rotation at subduction margins: How complexity at fault-scale (the 2019 Albanian M_w 6.4 earthquake) mirrors the regional deformation. *Terra Nova*, *00*, *1–9*. https://doi.org/10.1111/ter.12584